Assembly of nanocube super-structures directed by surface and magnetic interactions

Igor Stanković,*,† Luis Lizardi,‡ and Carlos García‡

†*Institute of Physics Belgrade, University of Belgrade, Pregrevica 118, 11080 Belgrade, Serbia.*

‡*Departamento de Física & Centro Científico Tecnológico de Valparaíso-CCTVal, Universidad Técnica Federico Santa María, Av. España 1680, Casilla 110-V, Valparaíso, Chile.*

E-mail: igor.stankovic@ipb.ac.rs

Magnetic field of [001] and [111] uniformly magnetised cubes

Magnetic nanoparticles can have complex coupling involving both dipolar and exchange interactions. The atomic exchange interaction is relevant up to a length scale of 10nm.[1] Thus, dipolar coupling dominates in the formation of the structures on the length scales 10nm-100μm, with many potential applications.[2–6] Due to shape anisotropy, small single domain magnets behave like uniaxial magnets. We characterize the system using dipole-dipole interaction potential: it is assumed that each particle carries identical dipolar (magnetic) moment with magnitude $M_0 = m_{\mathrm{s}} d^3$ where m_{s} is the magnetization and d the size of the cube. The analytic expressions for the magnetic field, of a sphere or an infinite cylinder, are part of classical magneto-static textbook.

For complex geometries we need to employ numerical solvers. Still, solution for bar magnet, deduced from the Maxwell equations can be also obtained analytically. For a magnetic

bar magnetized along the $y-$axis, i.e., $[010]$[7] one finds:

$$B_x^{[010]}(x,y,z) = \frac{\mu_0}{4\pi} M_0 \sum_{k,l,m=1}^{2} log[z + (-1)^m z_\mathrm{b} + A_\mathrm{sq}^{klm}] \tag{1}$$

$$B_y^{[010]}(x,y,z) = -\frac{\mu_0}{4\pi} M_0 \sum_{k,l,m=1}^{2} \frac{[y + (-1)^l y_\mathrm{b}][x + (-1)^k x_\mathrm{b}]}{|y + (-1)^l y_\mathrm{b}||x + (-1)^k x_\mathrm{b}|} \arctan\{\frac{|x + (-1)^k x_\mathrm{b}|[z + (-1)^m z_\mathrm{b}]}{|y + (-1)^l y_\mathrm{b}| A_\mathrm{sq}^{klm}}\} \tag{2}$$

$$B_z^{[010]}(x,y,z) = \frac{\mu_0}{4\pi} M_0 \sum_{k,l,m=1}^{2} log[x + (-1)^k x_\mathrm{b} + A_\mathrm{sq}^{klm}] \tag{3}$$

where $A_\mathrm{sq}^{klm} = \sqrt{[x + (-1)^k x_\mathrm{b}]^2 + [y + (-1)^l y_\mathrm{b}]^2 + [z + (-1)^m z_\mathrm{b}]^2}$.

For a bar magnetized along the $x-$axis, it is sufficient to rotate the system as follow: $B_x^{[100]}(x,y,z) = B_z^{[010]}(-y,x,z)$, $B_y^{[100]}(x,y,z) = -B_x^{[010]}(-y,x,z)$, and $B_z^{[100]}(x,y,z) = B_y^{[010]}(-y,x,z)$, and for a bar magnetized along the $z-$axis, $B_x^{[001]}(x,y,z) = B_x^{[010]}(x,z,-y)$, $B_y^{[001]}(x,y,z) = -B_z^{[010]}(x,z,-y)$, $B_z^{[001]}(x,y,z) = B_y^{[010]}(x,z,-y)$. Finally, the magnetic field of a cube ($x_\mathrm{b} = y_\mathrm{b} = z_\mathrm{b}$) magnetized along the principal diagonal (i.e., [111]), is the sum of the previous expressions, $\vec{B}^{[111]} = (\vec{B}^{[100]} + \vec{B}^{[010]} + \vec{B}^{[001]})/\sqrt{3}$.

Particle and square assembly

In order to gain a good understanding of dipolar interactions within an assembly of magnetic nanocubes, we will consider three relevant cases: (a) chain, (b) 5x5 square and (c) 5x5x5 cube. The chain, square, and super-cube have all anti-ferromagnetic order corresponding to their respective ground state configuration. We probe energy landscape experienced by a single [111] magnetised cube moving on top of these structures. An oscillatory chess-board landscape is reported here giving rise to alternating longitudinal attraction/repulsion upon shifting the cube. Thereby, the periodicity is essentially dictated by the cube size.

In more detail, the lowest energy is obtained for the front-right corner, see fig. S1. Then, upon shifting the cube away from the corner the cohesive energy at minimum is increasing. This first global minimum has similar depth in all three considered cases and, it is important

to note, the cubes centre of the mass is above the centre of the cube below. This latter point will be used in building the minimisation strategy described below. The alignment of the centres of the mass leads to the rectangular form of the minimal energy objects.

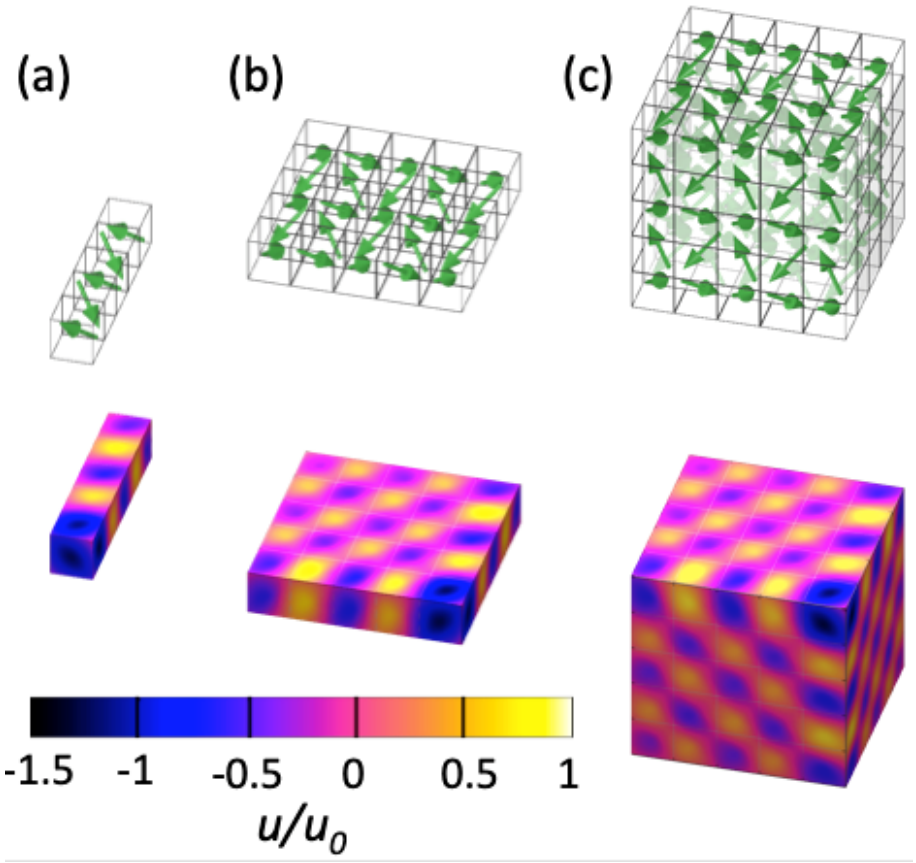

Figure S1: Energy landscape one uniformly [111] magnetised cube experiences over an assembly of magnetic cubes in ground state.

Analytic energy calculations

One way to obtain the state with lowest value is to calculate all possible magnetic configurations and geometrical configurations. This is also instructive since it gives also idea about energy differences between different states and especially between ground state and the first exited states. For $2 \leq N \leq 8$, we extensively surveyed the energies of all possible configurations and generated a database of energies. We visualised the obtained configuration's energy in terms of a geometric configuration in Fig. S2). The configuration are sorted and

indexed (x-axis) from lowest to highest energy for each geometric configuration separately. The energies are sorted in increasing order (on the abscissa is arbitrary index of the configuration), while the ordinate corresponds to the magnetic energy for a given configuration. The energies for different geometric configurations are given. The red curves in Fig. S2 correspond to the global geometric configuration, which is also a global minima for a given number of cubes. A linear chain structure (blue curve) is also found at higher energy for $N \geq 3$. The $N = 5$ is the first three dimensional ground state and also show two dimensional configuration (green curve). The number of possible magnetic configurations increases with 8^N scaling law so, with our computational resources, we follow this calculations up to $N \leq 8$.

In case of pure 40 nm[1] single-crystal magnetite cube and $M_\mathrm{s} = 160$ kA/m, *cf.* Ref.[8] Small single-domain magnets are treated like uniaxial magnets. Their interaction is described through dipole-dipole interaction potential: it is assumed that each particle carries identical dipolar (magnetic) moment with magnitude $M_0 = M_\mathrm{s} d^3$. We consider the two most common magnetisation directions: alongside [001] or along the principal diagonal [111] of the cube. Magnetic nanoparticles can have complex coupling involving both dipolar and exchange interactions. The reference magnetic interaction energy $\upsilon = \mu_0 M_0^2 / 4\pi d^3$ was estimated to be $\upsilon = 1$ eV.

Discrete dipole model for interaction of magnetic cubes

The previous analytic formula in Eq. 1-3 is applicable for the analytical analysis of dipolar interaction of cubes, but it is not practical for large number of particles ($N > 16$) and numeric optimization. We constructed a model which combines numerical precision with computational efficiency. The cubes are modelled as a cluster of hard spheres filling a cubical frame. A magnetic cube with side d is represented with nine spheres; a big sphere in the centre with radius $d/2$ and eight smaller spheres touching the inner corners of the cube. A cube, represented using a potential energy of interaction $U(\vec{r}_{ij})$ between pairs of

[1]We chose the cube's dimensions to facilitate comparison both with real units used in experiment and scaled used in generic theoretical considerations.

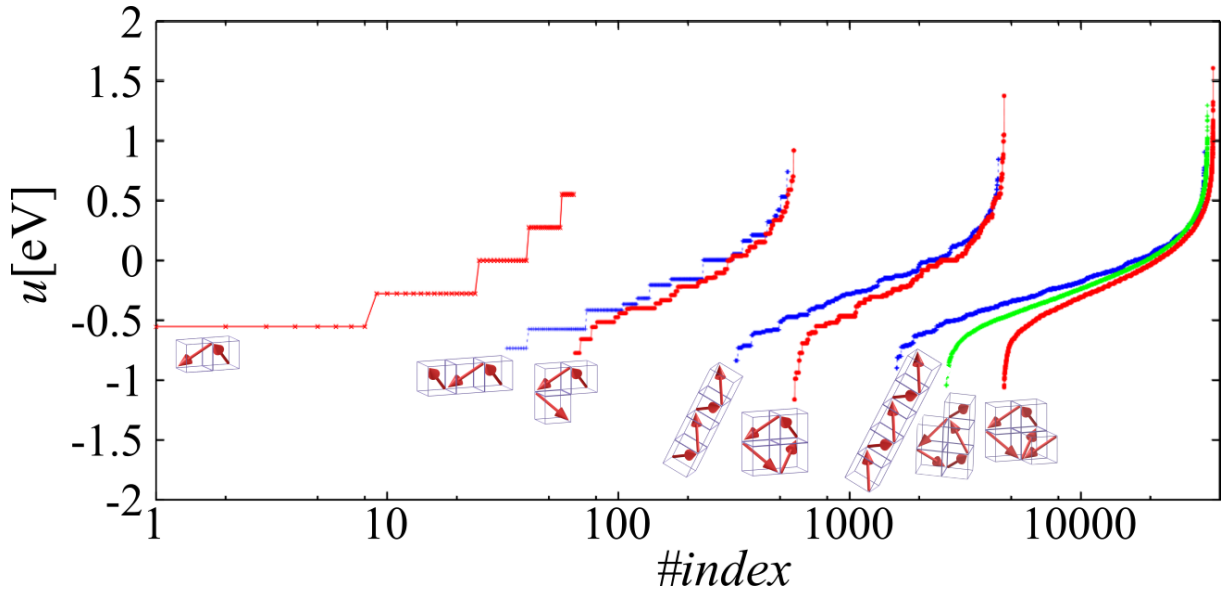

Figure S2: Energy profile showing the energy of all possible magnetic states for nanocubes magnetised along the principal diagonal [111] of the cube. The geometric configuration with lowest energy is represented in red. The configuration are sorted and indexed (x-axis) according to their energy to facilitate visualisation of the data. The energies are given in electron-volts, *i.e.*, the reference magnetic energy is $\upsilon = 1$ eV.

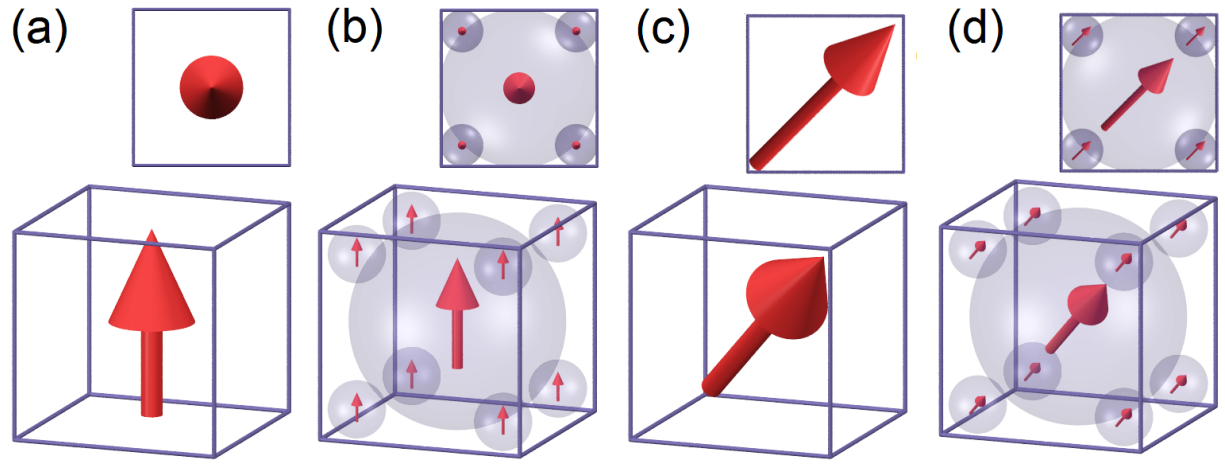

Figure S3: (a) Uniformly [001] magnetized magnetic cube, (b) nine dipole model for [001] magnetized cube, (c) uniformly [111] magnetized magnetic cube, (d) nine dipole model for [111] magnetized cube, and (e) mechanical contact model representation of the cube. Top (upper row) and side (lower row) view are given for comparison.

the point-like dipoles with the sphere centres located at $\vec{r}_i$ and $\vec{r}_j$, can be written as:

$$U_{\mathrm{m}}(\vec{r}_{ij}) = \frac{\mu_0}{4\pi}\left[\frac{\vec{m}_i \cdot \vec{m}_j}{r_{ij}^3} - 3\frac{(\vec{m}_i \cdot \vec{r}_{ij})(\vec{m}_j \cdot \vec{r}_{ij})}{r_{ij}^5}\right], \tag{4}$$

where $r_{ij} = |\vec{r}_{ij}| = |\vec{r}_j - \vec{r}_i|$, and $i, j = 1 \cdot 9$. In this model, the magnetic moment (m_i) carry a fraction of the total magnetic moment and it is expressed as $m_i = I^{\mathrm{s}} v_i$, where v_i is the volume of the magnetic part of the particle. The volume of the central particle is $v_1 = \pi/6$ and the volume of the smaller particles located at the corners is $v_{2\ldots9} = \pi(2-\sqrt{3})^3/6$. The magnetic density, which insures same energy between uniformly magnetised cubes placed on top of each other (minimal energy configuration) as in the case of uniformly magnetised cubes, is $I^{\mathrm{s}} \approx 2.1 \cdot M_0/d^3$. This magnetic density is independent of the investigated magnetisation directions, i.e., [001] and [111].

Using nine dipoles, we consider the interaction of the cube corners, which was not taken into account in the previously used models.[9] The main difference is observed in the position of the second maximum when the c.m. of one particle is on the corner of the other, see Fig. S6. While in single dipole model[9] the secondary peak (i.e., head-tail minimum) lies at $\Delta^1_{\mathrm{xy}}/\sqrt{2}d \approx 0.39$, in our nine dipole model is at $\Delta^9_{\mathrm{xy}}/\sqrt{2}d \approx 0.45$, significantly closer to the result for a uniformly magnetized cube $\Delta^{\mathrm{unif}}_{\mathrm{xy}}/\sqrt{2}d = 1/2$. The position of the secondary peak is important since it provides flexibility to the chain movement, i.e., particle at the corner can easily flip over the side to a similar energy state. Thereby, the total potential energy related to the magnetic interaction of two particles, with indices α, β in a given structure $U^{\mathrm{tot}}_{\mathrm{m}}$, is given by a sum over pairs of dipoles:

$$U^{\alpha\beta}_{\mathrm{m}} = \sum_{\substack{i,j=1..9 \\ i>j}} U_{\mathrm{m}}(\vec{r}^{\,\alpha\beta}_{ij}). \tag{5}$$

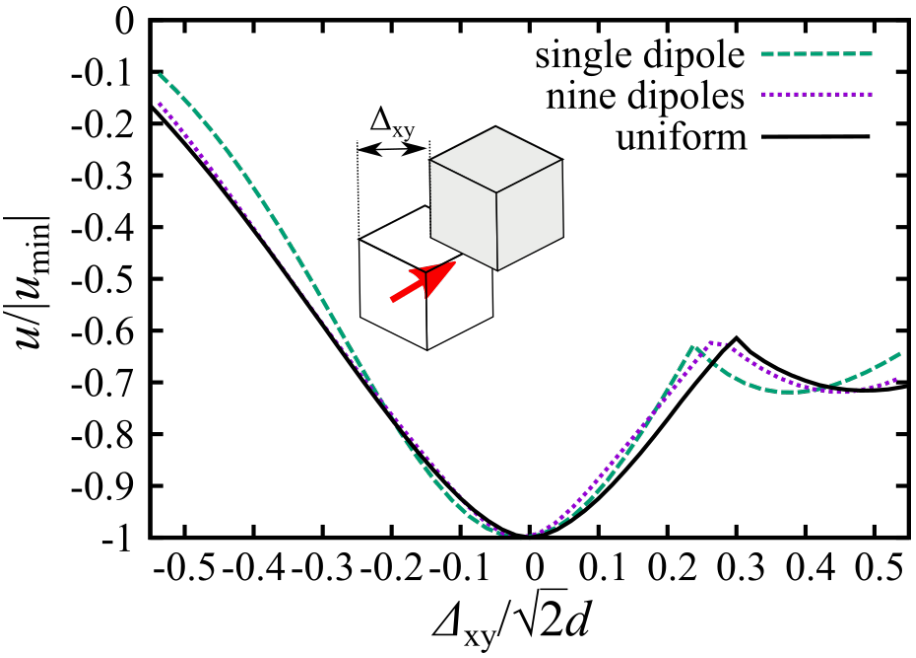

Figure S4: Comparison of the interaction energy of two uniformly magnetised cubes considering a nine-dipole and a single-dipole models.[9] The minimal energy for different positions along the diagonal of the cube are shown.

Genetic algorithm for minimisation ($N > 16$)

In numerical part of the work (i.e., Fig. 5 and 6), the reduced potential energy of interaction U_N has been minimised by evolving transient configurations on a square lattice using genetic algorithm.[10] In order to increase the chance of finding the ground state, we typically employ many independent populations of about 100 initial configurations consisting of individual particle position and magnetisation written in a so called genome of individual (i.e., individual configuration). If the particle is present or not on certain position on 3d lattice was registered with 1 or 0, respectively in corresponding part of genome. Also in other part of genome magnetisation of the particles is mapped on an array of 0-7 corresponding to eight possible magnetisation pointing from centre to one of the eight corners of the cube.

The evolution starts from a population of randomly generated individuals (i.e., configurations), and consists of an iterative process of creation of new generations. In each generation, the potential energy of interaction U_{tot} is evaluated for each individual in the population. The prime difference to usual deterministic minimisation procedures is that multiple indi-

viduals evolve in each step in a stochastic manner: A number of the best configurations are selected from the current population and modified (recombined and randomly mutated) to form the new generation. The algorithm terminates when a prescribed maximum number of generations has been produced and no more improvement of the best individual(s) is achieved.

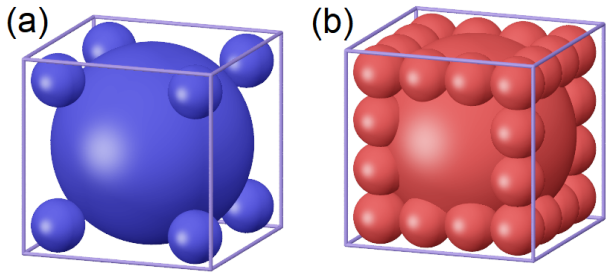

Figure S5: (a) nine dipole model for surface short-ranged repulsion/attraction interaction, and (b) contact potential model.

Discrete model for short-range surface interaction of cubes

Here we introduce surface repulsion or attraction model used in molecular dynamics simulations. It is a practical short-ranged model to be used for large number of particles and numeric optimisation. We constructed a model which is compatible with previously introduced nine dipole model, i.e., the cube is modelled as a cluster of hard spheres filling a cubical frame. The surface interaction is separated in two independent components (a) surface interaction proportional to contact area which can be attractive and repulsive and (b) contact interaction which is purely repulsive and prevents cubes from crossing each-other.

Just like in the nine dipole model, the contact area dependent surface interaction is modelled by replacing a cube with side d with nine spheres: a big sphere in the centre with radius $d/2$ and eight smaller spheres touching the inner corners of the cube, see Fig. S5a. A surface energy, represented using a potential energy of interaction $e_S(\vec{r}_{ij})$ between pairs of the point-like dipoles with the sphere centres located at $\vec{r}_i$ and $\vec{r}_j$. We have chosen Yukawa

potential form, written as:

$$e_{\mathrm{S}}(\vec{r}_{ij}) = \frac{\epsilon}{d} s_i s_j \frac{e^{\kappa r/d}}{r} \tag{6}$$

where ϵ, κ are energy and length parameters and $i, j = 1 \cdot 9$. The length parameter is set to $\kappa = 5$. In this model, every sphere models interaction with a fraction of the total surface it represents, i.e., $s_i = \pi d_i^2$, $d_i = 1/2, (2-\sqrt{3})d/2$.

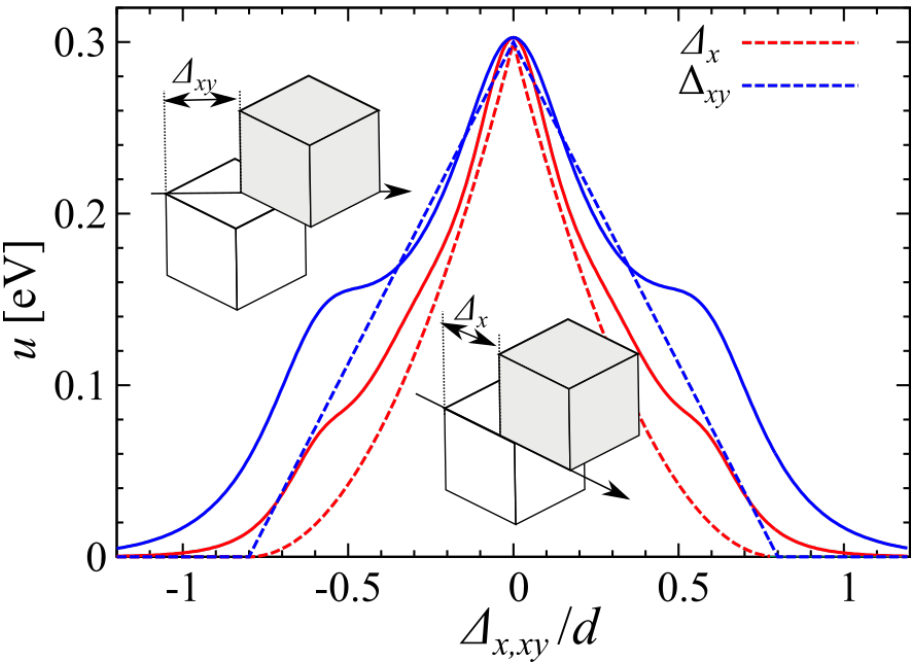

Figure S6: Comparison of the interaction energy of repulsive cubes considering a nine particles interacting with Yukawa potential form and repulsion proportional to contact surface. The energy profile of two systems is shown for displacement of centre of mass of two cubes along cube's edge Δ_x and face diagonal Δ_{xy} directions.

The energy profiles of contact area dependent repulsive surface interaction ($\epsilon > 0$) are compared with analytic calculations surface energy proportional to the contact surface in Fig. S6.

The contact potential of the cubes is represented by four overlapping spheres per edge with diameter radii $(2-\sqrt{3})d/2$, having a total of 32 spheres, and the central sphere with radius $d/2$, see Fig. S5b. These, in fact, cuboids are rigid bodies with fixed distances between spheres. This model is mainly chosen to prevent the geometric cube overlaps while at the same time creating a smooth and incommensurate surfaces allowing smooth gliding of one

cube over the other. The incommensurability is important since it prevents the system to mechanically lock in commensurable states and enables smooth gliding of one cube over the other. We describe the effect of isotropic contact interaction between the spherical particles using a minimal model, i.e., representing them by the soft-core beads. The spheres therefore interact isotropically by means of truncated at minima $r_{\rm cut} = 2^{1/6}\sigma$ and shifted Lennard-Jones potential, also known as Weeks-Chandler-Andersen (WCA) potential. The interaction is defined as: $U_{\rm LJ}^{\rm cut}(r) = U_{\rm LJ}(r) - U_{\rm LJ}(r_{\rm cut}), r < r_{\rm cut}$ and $U_{\rm cut} = 0, r \geq r_{\rm cut}$, where $r_{\rm cut}$ is the distance at which the potential is truncated, and $U_{\rm LJ}(r)$ is the conventional Lennard-Jones (LJ) potential, i.e., $U_{\rm LJ}(r) = -4\epsilon[(\sigma/r)^{12} - (\sigma/r)^{6}]$. The parameter ϵ corresponds to the energy scale of the interaction and σ is related to the characteristic diameter of the spheres δ. i.e., $\sigma = \delta/2^{1/6}$ and $\delta/d = 1$ and $(2-\sqrt{3})d$ for large and small spheres respectively. The value of the sphere repulsive contact potential is taken $\epsilon_r = 7 \cdot 10^{-16}$J for particles with the same $d = 25$nm size of the cube (i.e., $\epsilon_r = 800U_{\rm m}^{\alpha\beta}$).

Evolution of energy with temperature

Fig. S7 and S7 gives the calculated dependence of the intra-particle energy on the temperature. The intra-particle energy term includes magnetic and short-range surface interaction. In case of pure 80 nm and $M_{\rm s} = 18$ kA/m, *cf.* Ref.,[11] the reference magnetic interaction energy $\upsilon = \mu_0 M_0^2/4\pi d^3$ is estimated to be $\upsilon = 1$ eV which corresponds to 12000K reference temperature. The results are material and scale independent, the reference energy and temperature depend on particle size. For $d = 25$ nm is referent temperature is $\upsilon = 30$ meV and temperature 320K.

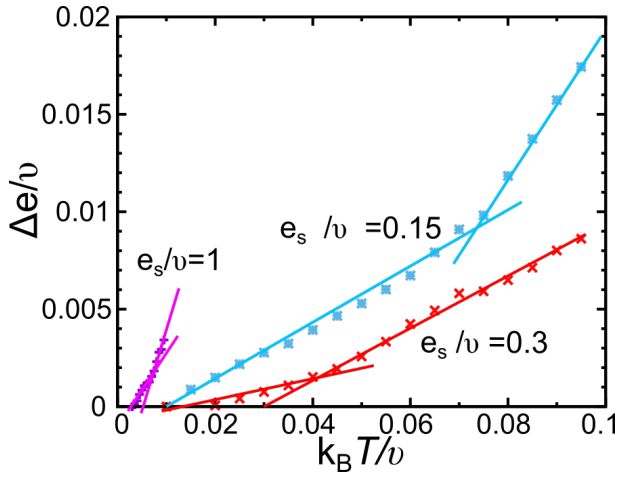

Figure S7: Increase of potential energy including magnetic and short-range surface interaction with temperature used to track the structural changes for a super-cube consisting of 216 nanocubes with [111] magnetisation. The results are shown for different repulsive surface couplings.

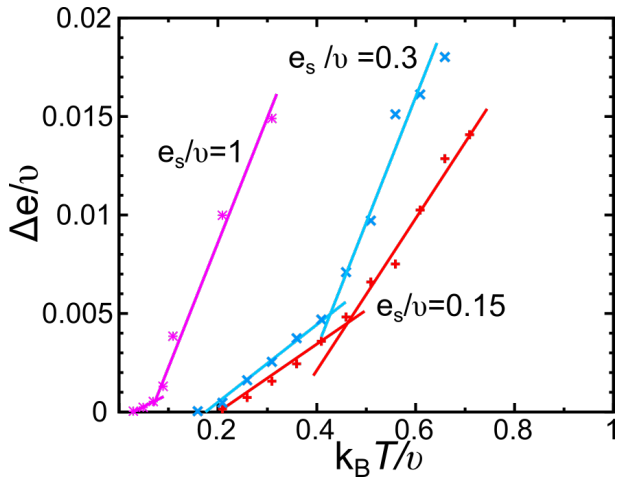

Figure S8: Increase of potential energy including magnetic and short-range surface interaction with temperature used to track the structural changes for a super-rod consisting of 128 nanocubes with [001] magnetisation. The results are shown for different repulsive surface couplings.

References

(1) Lin, X.-M.; Samia, A. C. Synthesis, assembly and physical properties of magnetic nanoparticles. *Journal of Magnetism and Magnetic Materials* **2006**, *305*, 100 – 109.

(2) Kuzyk, A.; Schreiber, R.; Fan, Z.; Pardatscher, G.; Roller, E.-M.; Hogele, A.; Simmel, F. C.; Govorov, A. O.; Liedl, T. DNA-based self-assembly of chiral plasmonic nanostructures with tailored optical response. *Nature* **2012**, *483*, 311–314.

(3) Zhang, Y.; Lu, F.; Yager, K. G.; van der Lelie, D.; Gang, O. A general strategy for the DNA-mediated self-assembly of functional nanoparticles into heterogeneous systems. *Nat Nano* **2013**, *8*, 865–872.

(4) Yan, J.; Bloom, M.; Bae, S. C.; Luijten, E.; Granick, S. Linking synchronization to self-assembly using magnetic Janus colloids. *Nature* **2012**, *491*, 578–581.

(5) Zhou, Y.; Shimizu, T. Lipid Nanotubes: A Unique Template To Create Diverse One-Dimensional Nanostructures. *Chemistry of Materials* **2008**, *20*, 625–633.

(6) Liu, X.; Marangon, I.; Melinte, G.; Wilhelm, C.; Ménard-Moyon, C.; Pichon, B. P.; Ersen, O.; Aubertin, K.; Baaziz, W.; Pham-Huu, C.; Bégin-Colin, S.; Bianco, A.; Gazeau, F.; Bégin, D. Design of Covalently Functionalized Carbon Nanotubes Filled with Metal Oxide Nanoparticles for Imaging, Therapy, and Magnetic Manipulation. *ACS Nano* **2014**, *8*, 11290–11304.

(7) Engel-Herbert, R.; Hesjedal, T. Calculation of the magnetic stray field of a uniaxial magnetic domain. *Journal of Applied Physics* **2005**, *97*, 074504.

(8) Niculaes, D.; Lak, A.; Anyfantis, G. C.; Marras, S.; Laslett, O.; Avugadda, S. K.; Cassani, M.; Serantes, D.; Hovorka, O.; Chantrell, R.; Pellegrino, T. Asymmetric Assembling of Iron Oxide Nanocubes for Improving Magnetic Hyperthermia Performance. *ACS Nano* **2017**, *11*, 12121–12133.

(9) Rossi, L.; Donaldson, J. G.; Meijer, J.-M.; Petukhov, A. V.; Kleckner, D.; Kantorovich, S. S.; Irvine, W. T. M.; Philipse, A. P.; Sacanna, S. Self-organization in dipolar cube fluids constrained by competing anisotropies. *Soft Matter* **2018**, *14*, 1080–1087.

(10) Messina, R.; Stanković, I. Assembly of magnetic spheres in strong homogeneous magnetic field. *Physica A: Statistical Mechanics and its Applications* **2017**, *466*, 10 – 20.

(11) Abenojar, E. C.; Wickramasinghe, S.; Ju, M.; Uppaluri, S.; Klika, A.; George, J.; Barsoum, W.; Frangiamore, S. J.; Higuera-Rueda, C. A.; Samia, A. C. S. Magnetic glycol chitin-based hydrogel nanocomposite for combined thermal and D-amino-acid-assisted biofilm disruption. *ACS infectious diseases* **2018**, *4*, 1246–1256.